

***AstroSat* investigation of X-ray flares on two active K-M systems: CC Eri and AB Dor**

Subhajeet KARMAKAR^{1,*}, Jeewan C. PANDEY², Nikita RAWAT², Gurpreet SINGH²
and Riddhi SHEDGE^{1,3}

¹ Monterey Institute for Research in Astronomy (MIRA), 200 Eighth Street, Marina, California 93933, USA

² Aryabhata Research Institute of Observational Sciences (ARIES), Manora Peak, Nainital 263002, India

³ Monta Vista High School, 21840 McClellan Rd, Cupertino, CA 95014, USA

* Corresponding author: subhajeet09@gmail.com, sk@mira.org

Abstract

We present an X-ray and UV investigation of five X-ray flares detected on two active systems, CC Eri and AB Dor, using the *AstroSat* observatory. The peak X-ray luminosities of the flares in the 0.3–7.0 keV band are found to be within 10^{31-33} erg s⁻¹. Preliminary spectral analysis indicates the presence of three and four-temperature corona for CC Eri and AB Dor, respectively, where the highest temperature is found to vary with flare. The flare temperatures peaked at 51–59 MK for CC Eri and 29–44 MK for AB Dor. The peak emission measures of the flaring loops are estimated to be $\sim 10^{54}$ for CC Eri and $\sim 10^{55}$ cm⁻³ for AB Dor. Global metallic abundances were also found to increase during flares.

Keywords: stars: activity, stars: coronae, stars: flare, AB Dor, CC Eri, stars: low-mass, stars: magnetic field.

1. Introduction

Solar-type stars with a convective envelope above a radiative interior show a high level of magnetic activity (Patel et al., 2016; Karmakar et al., 2018, 2019; Savanov et al., 2018b). Binaries and multiple systems are even more magnetically active due to the large influence of the rotation of the individual stars by tidal interactions. Understanding the magnetic activities are very important as they provide useful information about the stellar dynamo theory and stellar spaceweather (Maehara et al., 2012; Karmakar, 2021).

Stellar flares are extreme dynamic behavior of the stellar atmosphere and are an important manifestation of magnetic activities (Pandey and Karmakar, 2015; Savanov et al., 2018a; Karmakar and Pandey, 2018; Karmakar et al., 2016, 2022b, 2023). In this paper, we investigated two highly active systems CC Eri and AB Dor observed with *AstroSat* satellite. CC Eri is a K7.5+M3.5 binary located at a distance of ~ 11.5 pc, whereas AB Dor is known to be a

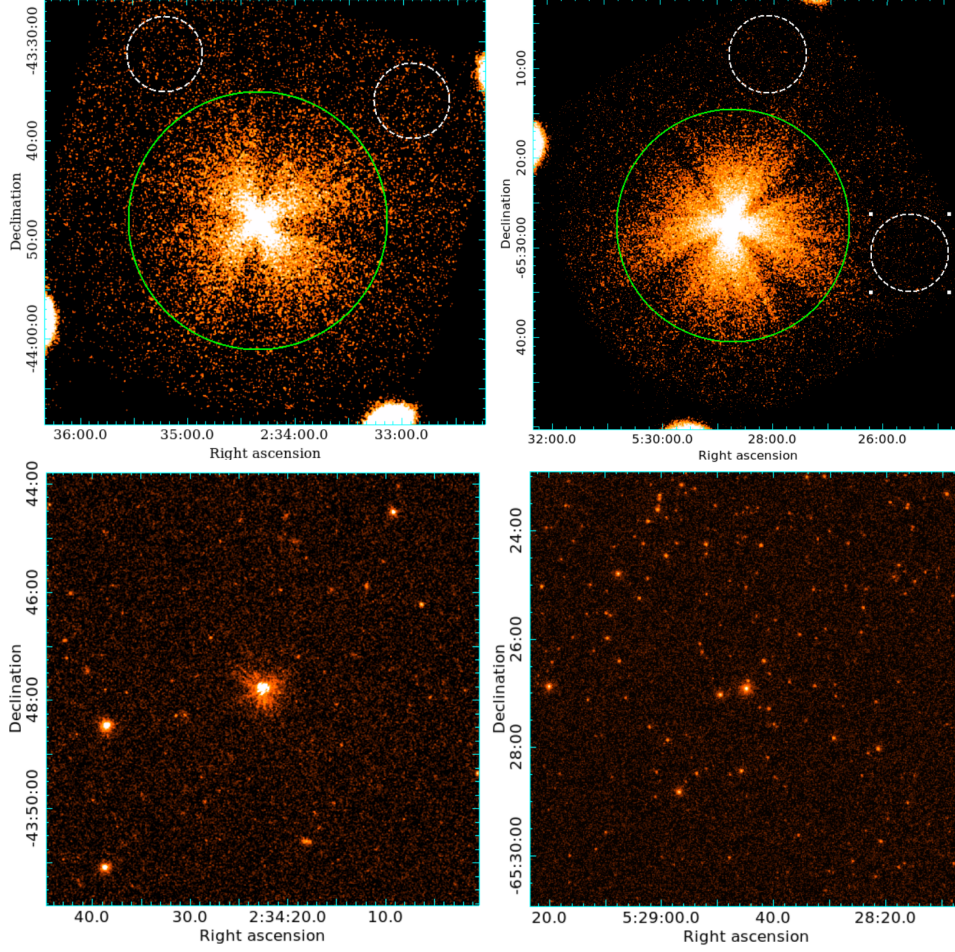


Figure 1: *AstroSat* X-ray and UV images. In the top panel, the soft X-ray Images of CC Eri (left) and AB Dor (right) are shown. In the bottom panel, the near-ultraviolet (NUV) images of CC Eri (left) and far-ultraviolet (FUV) images of AB Dor (right) are shown with the sources placed at the center. The selected source and background regions in the top panels are shown with green circles and white dashed circles, respectively.

K0+M8+M5+M5-6 quadrupole system located at ~ 14.9 pc (Bailer-Jones et al., 2018). Both the objects showed variations in X-ray and UV, and multiple flaring activities have been observed (Crespo-Chac3n et al., 2007; Karmakar et al., 2017; Karmakar, 2019; Didel et al., 2022). Using the simultaneous observations in UV and X-ray, our objective is to investigate the coronal and chromospheric features of the systems.

We structured the paper as follows: Section 2 describes the observations and data reduction. Analysis and results from X-ray timing and spectral analysis are presented in Section 3. Finally, in Section 4, we discuss the result and present conclusions.

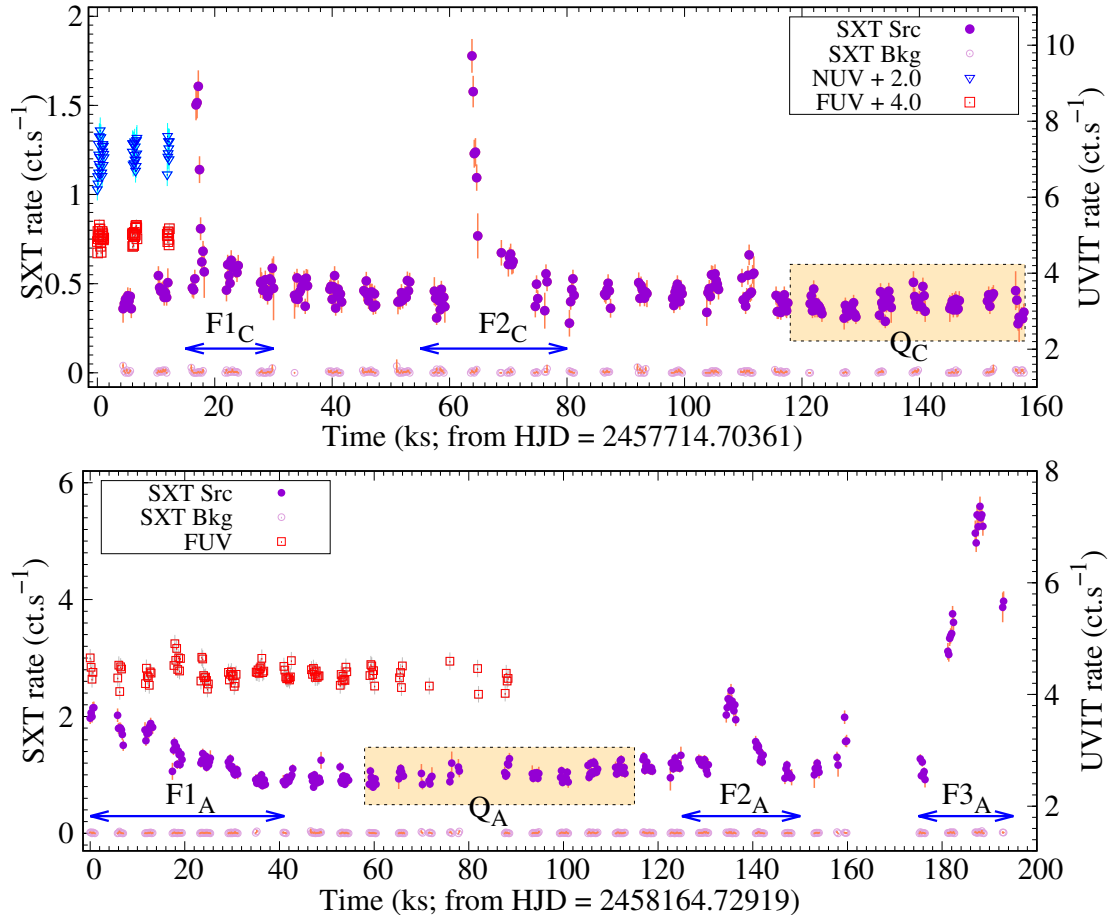


Figure 2: X-ray and UV light curves from *AstroSat* SXT (left Y-axis) and UVIT (right Y-axis) have been shown. The top and bottom panel shows the background subtracted light curves of CC Eri and AB Dor, respectively, along with the background light curves for each observation. The arrows show the identified flare duration, whereas the yellow-shaded regions indicate the quiescent corona.

2. Observations and Data Reduction

We observed CC Eri and AB Dor using Soft X-ray focusing Telescope (SXT; Singh et al., 2014, 2017), Large Area X-ray Proportional Counter (LAXPC; Antia et al., 2017), Cadmium Zinc Telluride Imager (CZTI; Bhalerao et al., 2017), and Ultra-Violet Imaging Telescope (UVIT; Tandon et al., 2017) onboard *AstroSat* observatory, on 2016 November 22 (PI. Karmakar; ID: A02_151T01_9000000818) and 2018 February 15 (PI. Karmakar; ID: A04_116T01_9000001896), respectively. In this article, we only report the results obtained by the SXT and UVIT instruments.

CC Eri and AB Dor were observed in an energy range of 0.3–7 keV with SXT for a stare time of ~ 160 and ~ 200 ks. The level 1 data were processed using the `AS1SXTLevel2-1.4b` pipeline software to produce level 2 clean event files for each orbit of observation. Each event file corresponding to each orbit was merged to a single cleaned event file using the `sxtevtmerger` tool. In order to extract images, light curves, and spectra, we used the `FTOOLS`

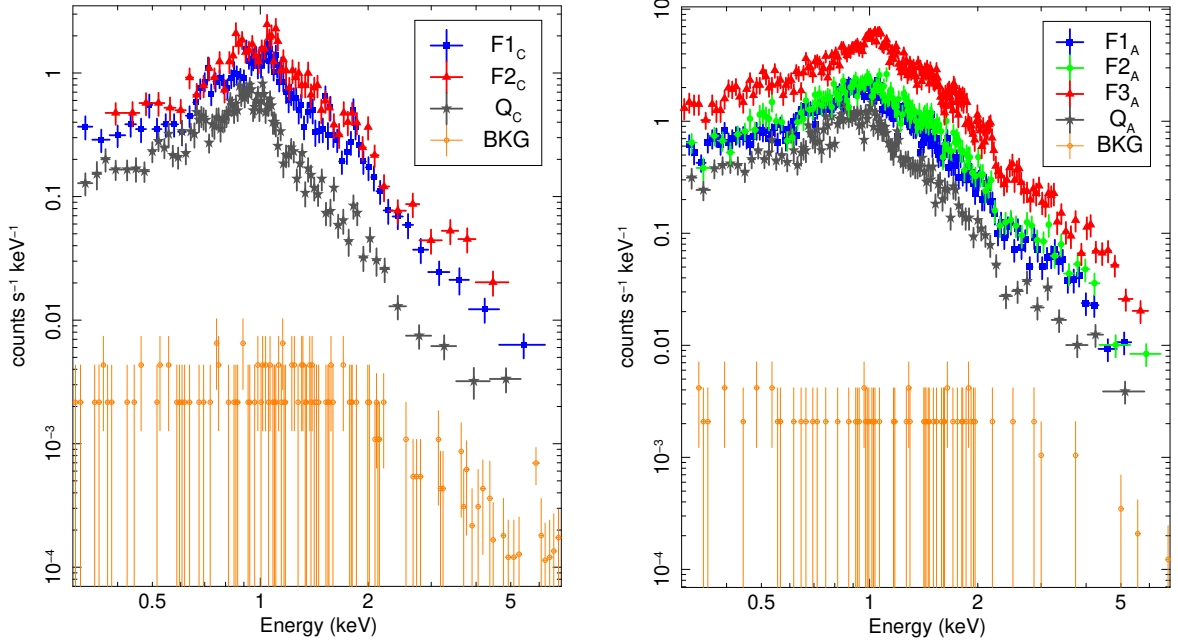


Figure 3: The time-resolved *AstroSat*/SXT spectra for CC Eri (left) and AB Dor (right), along with the background spectra are shown. Different colors indicate the spectra correspond to different time segments, as shown in Figure 2, whereas the background spectra are obtained from the complete observations.

task `xselect` V3.5, which has been provided as a part of the `heasoft` version 6.30. Due to the broad PSF of *AstroSat* SXT ($2'$ inner and $10'$ – $12'$ outer King’s profile), we have chosen a circular region of a radius of $13'$ centered at the source position to extract source products. We carefully verified that the region $\approx 17'$ – $19'$ from the sources are not affected by the source brightness and can safely be considered as background. We, therefore, have chosen multiple circular regions of 2.6 radii as background regions and shown in Figure 1. The background light curves, as shown in Figure 2, do not indicate any variation with the source. A similar background selection method was also followed by [Karmakar et al. \(2022a\)](#). The spectral analysis was carried out in an energy range of 0.3 – 7 keV using the X-ray spectral fitting package (`xspec`; version 12.11.1 [Arnaud, 1996](#)). For analysis of UVIT data and to extract the FUV and NUV light curve, we used the open-source `curvit` python package ([Joseph et al., 2021](#)).

3. Analysis and Results

The background subtracted 0.3 – 7 keV X-ray light curves of CC Eri (top panel) and AB Dor (bottom panel) along with the background light curves are shown in Figure 2. The source light curves show a large variation in SXT count rates from 0.4 to 1.8 count s^{-1} for CC Eri, and 0.8 to 5.8 count s^{-1} for AB Dor. From SXT light curves we detected two flaring events for CC Eri (F1_C and F2_C) and three flaring events are identified for AB Dor (F1_A, F2_A, and F3_A). In Figure 2, the UV light curves are also shown in the right-hand Y-axis. For CC Eri, both FUV and NUV observations were available, whereas AB Dor has been observed only in FUV.

Unfortunately, both UV observation does not cover the whole observation time. For CC Eri, the observation was interrupted by *Bright Object Dection* (BOD) phenomena at the onset of flare F1_C, whereas the interruption in UV observation for AB Dor might be due to some technical difficulty. The FUV and NUV light curve for CC Eri and FUV light curve for AB Dor are found to remain constant within 1σ uncertainty level.

We performed time-resolved spectroscopy for both sources with 11 segments for CC Eri and 25 segments for AB Dor. In Figure 3, we have shown the spectra of the quiescent state, the peak of each flare, and the background region for both observations. The background spectra show a similar pattern and background fluxes are multiple-order fainter than the quiescent spectra of the individual stars. The stellar X-ray spectra have been analyzed with *Astrophysical Plasma Emission Code* (APEC; [Smith et al., 2001](#)), assuming the bremsstrahlung continuum and adopting the emission lines from the latest *Astrophysical Emission Database*. Preliminary spectral analysis indicates the presence of three and four-temperature corona for CC Eri and AB Dor, respectively, where the highest temperature is found to vary with flare. The flare temperatures peaked at 51–59 MK for CC Eri and 29–44 MK for AB Dor. The peak emission measures of the flaring loops are estimated to be $\sim 10^{54}$ for CC Eri and $\sim 10^{55} \text{ cm}^{-3}$ for AB Dor. Global metallic abundances were found to vary with flare. The peak X-ray luminosities of the flares are found to be within $10^{31-33} \text{ erg s}^{-1}$.

4. Discussion and Conclusion

In this paper, we have investigated two active stars with the *AstroSat* observatory. A total of five flaring events have been detected. Although the stellar flares are spatially resolved, it is possible to infer the physical size and structure of the flares using the loop models. Assuming a semi-circular constant cross-section loop, the coronal loop height, plasma density, and the loop aspect ratio can be estimated using the quasi-static loop modeling ([Van den Oord and Mewe, 1989](#)). Further investigation on the coronal loop properties and associated dynamo mechanisms is being carried out and will be presented elsewhere.

Acknowledgments

This publication uses data from the *AstroSat* mission of ISRO, archived at the Indian Space Science Data Centre (ISSDC). We thank the SXT Payload Operation Center at TIFR, Mumbai, for providing the necessary software tools. This research has used the software provided by the High Energy Astrophysics Science Archive Research Center (HEASARC), which is a service of the Astrophysics Science Division at NASA/GSFC.

Further Information

ORCID identifiers of the authors

0000-0001-8620-4511 (Subhajeet KARMAKAR)

0000-0002-4331-1867 (Jeewan C. PANDEY)

0000-0002-4633-6832 (Nikita RAWAT)

0009-0002-6580-3931 (Gurpreet SINGH)

0000-0002-2489-5908 (Riddhi SHEDGE)

Author contributions

All authors have significantly contributed to this paper.

Conflicts of interest

The authors declare no conflict of interest.

References

- Antia, H. M., Yadav, J. S., Agrawal, P. C., Verdhhan Chauhan, J., Manchanda, R. K., Chitnis, V., Paul, B., Dedhia, D., Shah, P., Gujar, V. M., Katoch, T., Kurhade, V. N., Madhwani, P., Manojkumar, T. K., Nikam, V. A., Pandya, A. S., Parmar, J. V., Pawar, D. M., Pahari, M., Misra, R., Navalgund, K. H., Pandiyan, R., Sharma, K. S. and Subbarao, K. (2017) Calibration of the Large Area X-Ray Proportional Counter (LAXPC) Instrument on board AstroSat. *ApJS*, 231(1), 10. <https://doi.org/10.3847/1538-4365/aa7a0e>.
- Arnaud, K. A. (1996) XSPEC: The First Ten Years. In *Astronomical Data Analysis Software and Systems V*, edited by Jacoby, G. H. and Barnes, J., vol. 101 of *ASPC*, p. 17.
- Bailer-Jones, C. A. L., Rybizki, J., Fouesneau, M., Mantelet, G. and Andrae, R. (2018) Estimating Distance from Parallaxes. IV. Distances to 1.33 Billion Stars in Gaia Data Release 2. *AJ*, 156, 58. <https://doi.org/10.3847/1538-3881/aacb21>.
- Bhalerao, V., Bhattacharya, D., Vibhute, A., Pawar, P., Rao, A. R., Hingar, M. K., Khanna, R., Kutty, A. P. K., Malkar, J. P., Patil, M. H., Arora, Y. K., Sinha, S., Priya, P., Samuel, E., Sreekumar, S., Vinod, P., Mithun, N. P. S., Vadawale, S. V., Vagshette, N., Navalgund, K. H., Sarma, K. S., Pandiyan, R., Seetha, S. and Subbarao, K. (2017) The Cadmium Zinc Telluride Imager on AstroSat. *JApA*, 38(2), 31. <https://doi.org/10.1007/s12036-017-9447-8>.
- Crespo-Chacón, I., Micela, G., Reale, F., Caramazza, M., López-Santiago, J. and Pillitteri, I. (2007) X-ray flares on the UV Ceti-type star CC Eridani: a “peculiar” time-evolution of spectral parameters. *A&A*, 471, 929–939. <https://doi.org/10.1051/0004-6361:20077601>.
- Didel, S., Pandey, J. C., Srivastava, A. K., Singh, G. and Karmakar, S. (2022) X-Ray Analysis of Two Highly Energetic Flares from AB Dor Observed by XMM-Newton. In *Cambridge Workshop on Cool Stars, Stellar Systems, and the Sun, Cambridge Workshop on Cool Stars, Stellar Systems, and the Sun*, p. 179. <https://doi.org/10.5281/zenodo.7588958>.

- Joseph, P., Stalin, C. S., Tandon, S. N. and Ghosh, S. K. (2021) Curvit: An open-source Python package to generate light curves from UVIT data. *JApA*, 42(2), 25. <https://doi.org/10.1007/s12036-020-09680-5>.
- Karmakar, S. (2019) Evolution of magnetic activities in Late-type stars. Ph.D. thesis, ARIES, Nainital, India; PRSU, Raipur, India. <https://doi.org/10.5281/zenodo.5762548>.
- Karmakar, S. (2021) How safe are we from gigantic Superflare on the Sun? *MIRA Newsletter*, 44(4), 3–5. <https://doi.org/10.5281/zenodo.5774473>.
- Karmakar, S., Naik, S., Pandey, J. C. and Savanov, I. S. (2022a) AstroSat observations of long-duration X-ray superflares on active M-dwarf binary EQ Peg. *MNRAS*, 509(3), 3247–3257. <https://doi.org/10.1093/mnras/stab3099>.
- Karmakar, S., Naik, S., Pandey, J. C. and Savanov, I. S. (2023) Swift and XMM-Newton observations of an RS CVn-type eclipsing binary SZ Psc: superflare and coronal properties. *MNRAS*, 518(1), 900–918. <https://doi.org/10.1093/mnras/stac2970>.
- Karmakar, S. and Pandey, J. C. (2018) An F-type ultra-fast rotator KIC 6791060: Starspot modulation and Flares. *BSRSL*, 87, 163–166. <https://doi.org/10.48550/arXiv.1805.08488>.
- Karmakar, S., Pandey, J. C., Airapetian, V. S. and Misra, K. (2017) X-Ray Superflares on CC Eri. *ApJ*, 840(2), 102. <https://doi.org/10.3847/1538-4357/aa6cb0>.
- Karmakar, S., Pandey, J. C., Naik, S., Savanov, I. S. and Raj, A. (2019) Magnetic activities on active solar-type stars. *BSRSL*, 88, 182–189. <https://doi.org/10.48550/arXiv.1905.13512>.
- Karmakar, S., Pandey, J. C., Savanov, I. S., Raj, A., Dmitrienko, E. S., Pakhomov, Y. and Sahu, D. K. (2018) Four years of starspot evolution on an active F-type ultra-fast rotator KIC 6791060. *IAUS*, 340, 229–232. <https://doi.org/10.1017/S1743921318001175>.
- Karmakar, S., Pandey, J. C., Savanov, I. S., Taş, G., Pandey, S. B., Misra, K., Joshi, S., Dmitrienko, E. S., Sakamoto, T., Gehrels, N. and Okajima, T. (2016) LO Peg: surface differential rotation, flares, and spot-topographic evolution. *MNRAS*, 459(3), 3112–3129. <https://doi.org/10.1093/mnras/stw855>.
- Karmakar, S., Reale, F., Morenzi, J. and Pandey, J. C. (2022b) NICER and Swift observations of X-ray Superflares on active RS CVn-type binary UX Ari. In *BAAS*, vol. 54, p. 6.
- Maehara, H., Shibayama, T., Notsu, S., Notsu, Y., Nagao, T., Kusaba, S., Honda, S., Nogami, D. and Shibata, K. (2012) Superflares on solar-type stars. *Nature*, 485, 478–481. <https://doi.org/10.1038/nature11063>.
- Pandey, J. C. and Karmakar, S. (2015) An X-Ray Flare from 47 Cas. *AJ*, 149, 47. <https://doi.org/10.1088/0004-6256/149/2/47>.
- Patel, M. K., Pandey, J. C., Karmakar, S., Srivastava, D. C. and Savanov, I. S. (2016) Broad-band linear polarization in late-type active dwarfs. *MNRAS*, 457, 3178–3190. <https://doi.org/10.1093/mnras/stw195>.

- Savanov, I. S., Dmitrienko, E. S., Karmakar, S. and Pandey, J. C. (2018a) Activity of Young Dwarfs with Planetary Systems: EPIC 211901114 and K2-33. *ARep*, 62, 532–541. <https://doi.org/10.1134/S1063772918080073>.
- Savanov, I. S., Dmitrienko, E. S., Pandei, D. S. and Karmakar, S. (2018b) On the Differential Rotation of Stars. *AstBu*, 73, 454–462. <https://doi.org/10.1134/S1990341318040077>.
- Singh, K. P., Stewart, G. C., Westergaard, N. J., Bhattacharayya, S., Chandra, S., Chitnis, V. R., Dewangan, G. C., Kothare, A. T., Mirza, I. M., Mukerjee, K., Navalkar, V., Shah, H., Abbey, A. F., Beardmore, A. P., Kotak, S., Kamble, N., Vishwakarama, S., Pathare, D. P., Risbud, V. M., Koyand e, J. P., Stevenson, T., Bicknell, C., Crawford, T., Hansford, G., Peters, G., Sykes, J., Agarwal, P., Sebastian, M., Rajarajan, A., Nagesh, G., Narendra, S., Ramesh, M., Rai, R., Navalgund, K. H., Sarma, K. S., Pandiyan, R., Subbarao, K., Gupta, T., Thakkar, N., Singh, A. K. and Bajpai, A. (2017) Soft X-ray Focusing Telescope Aboard AstroSat: Design, Characteristics and Performance. *JApA*, 38(2), 29. <https://doi.org/10.1007/s12036-017-9448-7>.
- Singh, K. P., Tandon, S. N., Agrawal, P. C., Antia, H. M., Manchanda, R. K., Yadav, J. S., Seetha, S., Ramadevi, M. C., Rao, A. R., Bhattacharya, D., Paul, B., Sreekumar, P., Bhattacharyya, S., Stewart, G. C., Hutchings, J., Annapurni, S. A., Ghosh, S. K., Murthy, J., Pati, A., Rao, N. K., Stalin, C. S., Girish, V., Sankarasubramanian, K., Vadawale, S., Bhalerao, V. B., Dewangan, G. C., Dedhia, D. K., Hingar, M. K., Katoch, T. B., Kothare, A. T., Mirza, I., Mukerjee, K., Shah, H., Shah, P., Mohan, R., Sangal, A. K., Nagabhusana, S., Sriram, S., Malkar, J. P., Sreekumar, S., Abbey, A. F., Hansford, G. M., Beardmore, A. P., Sharma, M. R., Murthy, S., Kulkarni, R., Meena, G., Babu, V. C. and Postma, J. (2014) ASTROSAT mission. In *Space Telescopes and Instrumentation 2014: Ultraviolet to Gamma Ray*, edited by Takahashi, T., den Herder, J.-W. A. and Bautz, M., vol. 9144 of *SPIE*, p. 91441S. <https://doi.org/10.1117/12.2062667>.
- Smith, R. K., Brickhouse, N. S., Liedahl, D. A. and Raymond, J. C. (2001) Collisional Plasma Models with APEC/APED: Emission-Line Diagnostics of Hydrogen-like and Helium-like Ions. *ApJ*, 556, L91–L95. <https://doi.org/10.1086/322992>.
- Tandon, S. N., Subramaniam, A., Girish, V., Postma, J., Sankarasubramanian, K., Sriram, S., Stalin, C. S., Mondal, C., Sahu, S., Joseph, P., Hutchings, J., Ghosh, S. K., Barve, I. V., George, K., Kamath, P. U., Kathiravan, S., Kumar, A., Lancelot, J. P., Leahy, D., Mahesh, P. K., Mohan, R., Nagabhushana, S., Pati, A. K., Kameswara Rao, N., Sreedhar, Y. H. and Sreekumar, P. (2017) In-orbit Calibrations of the Ultraviolet Imaging Telescope. *AJ*, 154(3), 128. <https://doi.org/10.3847/1538-3881/aa8451>.
- Van den Oord, G. H. J. and Mewe, R. (1989) The X-ray flare and the quiescent emission from Algol as detected by EXOSAT. *A&A*, 213, 245–260.